Available online at www.sciencedirect.com
SCIENCE DIRECT®
C. R. Physique 6 (2005) 1099–1109
COMPTES RENDUS PHYSIQUE
http://france.elsevier.com/direct/COMREN/

MCAO for very large telescopes/OAMC pour les très grands télescopes

Ground Layer Adaptive Optics

Norbert Hubin [a,*], Robin Arsenault [a], Ralf Conzelmann [a], Bernard Delabre [a], Miska Le Louarn [a], Stefan Stroebele [a], Remko Stuik [b]

[a] *European Southern Observatory, Karl Schwarzschild Strasse 2, 85748 Garching Bei München, Germany*
[b] *Leiden Observatory, P.O. Box 9513, NL-2300 RA, Leiden, The Netherlands*

Abstract

We will introduce the present knowledge of the turbulence profile C_n^2 and in particular we will emphasise the existence of a turbulence layer close to the ground. Then we will present the concept of Ground Layer Adaptive Optics and will provide estimates of performance expected from such systems and their potential for astronomical applications. Finally we will provide practical implementation concepts for two instruments at the VLT, MUSE and HAWK-I using multi-Laser Guide Stars and a large Deformable Secondary Mirror. The latter will also be described as its use is optimum for GLAO systems. ***To cite this article: N. Hubin et al., C. R. Physique 6 (2005).***

Résumé

Correction de la couche atmosphérique basse altitude par Optique Adaptative. Dans cet article, la connaissance du profile de turbulence et l'importance de la couche atmosphérique de sol est présentée. Le concept d'Optique Adaptative (OA) de sol, les performances ainsi que l'intérêt de ce type de système pour l'astronomie sont décrits.

Deux systèmes d'OA pour deux instruments, MUSE et HAWK-I du « Very Large Telescope » et basé sur ce concept sont présentés. Ces systèmes utilisent des étoiles artificielles lasers multiples ainsi qu'un miroir secondaire adaptatif de grand diamètre. L'intérêt de ce dernier pour ce type d'application ainsi que la description de son concept sont donnés. ***Pour citer cet article : N. Hubin et al., C. R. Physique 6 (2005).***

Keywords: Adaptive Optics; Ground Layer Adaptive Optics; Laser Guide Star; Laser Tomography; Turbulence profile; Ensquared Energy; Point Spread Function; Deformable secondary mirror; GRAAL; GALACSI; MUSE; HAWK-I; ASSIST

Mots-clés : Optique Adaptative ; Correction de la couche atmosphérique basse altitude ; Étoile artificielle laser ; Tomographie laser ; Profile de turbulence ; Énergie encerclée ; Fonction d'Etalement de Point ; Miroir secondaire déformable ; GRAAL ; GALACSI ; MUSE ; HAWK-I ; ASSIST

1. Introduction

Adaptive Optics (AO) systems developed over the last 30 years aimed at providing diffraction limited images of the telescopes usually for relatively bright sources – mv < 13–14 – and over a Field of View (FoV) reduced by the so-called

* Corresponding author.
E-mail address: nhubin@eso.org (N. Hubin).

1631-0705/$ – see front matter
doi:10.1016/j.crhy.2005.10.005

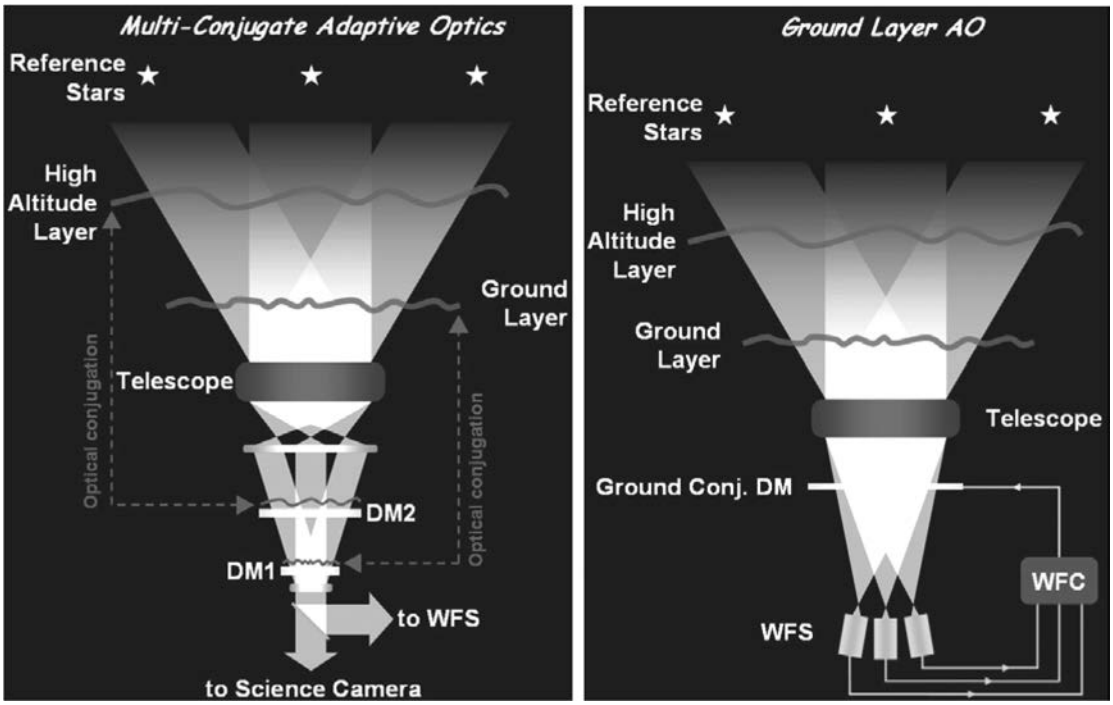

Fig. 1. Left: concept of multi-conjugate adaptive optics; Right: concept of ground layer adaptive optics.

anisoplanatism angle (30″ in the near IR, 2″ in the visible). Reference star brightness and limited corrected FoV have dramatically limited the part of the sky where the correction was possible – or sky coverage – and therefore has restricted the application of Adaptive Optics to stellar astronomy.

To increase the sky coverage, the concept of Laser Guide Star (LGS) was introduced (Foy and Labeyrie [1]) but the corrected FoV was still limited with in addition the introduction of a new limitation: the focus anisoplanatism or cone effect.

To overcome the cone effect, the concept of tomography using several LGSs for wavefront sensing (Tallon and Foy [2]) was proposed and to increase the corrected FoV the concept of Multi-Conjugate Adaptive Optics (MCAO) using several Deformable Mirrors (DM) conjugated to different atmospheric altitudes was introduced (Beckers [3]), (Ellerbroek [4]), (Johnston and Welsh [5]) and (Ragazzoni, Marchetti, Rigaut [6]); see Fig. 1.

Although MCAO and multi LGSs tomography wavefront sensing seems to be ideal – apart from the sky coverage partially limited by the need for a Natural Guide Stars (NGS) for the local LGS tilt correction over the FoV – in reality the complexity and cost of an MCAO increases rapidly with the requirements:

- Number of DMs depends on the corrected FoV and on the desired residual rms phase error (Tokovinin, Le Louarn and Sarazin [7]).
- Number, type of LGSs – Sodium or Rayleigh – and on-sky power depends on the residual phase error.

As an example, GEMINI MCAO system, optimised for a NIR corrected FoV of 2′, uses 3 DMs, 5 LGSs and 3 NGSs (Ellerbroek et al. [8]).

Based on this, science cases have been re-discussed with the astronomers and interest for partial AO correction was identified as promising for extra-galactic observations and cosmology.

It had been known for a long time that a strong turbulence layer usually exists close to the ground called ground or boundary layer (e.g. Vermin and Munoz-Tunon [9]). This layer shows a large anisoplanatism angle. A model of the vertical distribution of atmospheric turbulence, C_n^2 was obtained by discretizing into eight layers a profile obtained by a balloon sounding at Paranal – flight 52 from Le Louarn et al. [10] – and Cerro Pachon (Rigaut [11]) and a study about a portable turbulence profiler MASS was initiated by ESO (Tokovinin and Kornilov [12]). The latter was motivated by the MCAO research activities which called for a better statistical knowledge of the C_n^2 profiles to determine the best conjugation altitude for the MCAO DMs and the altitude variability of the main turbulent layers.

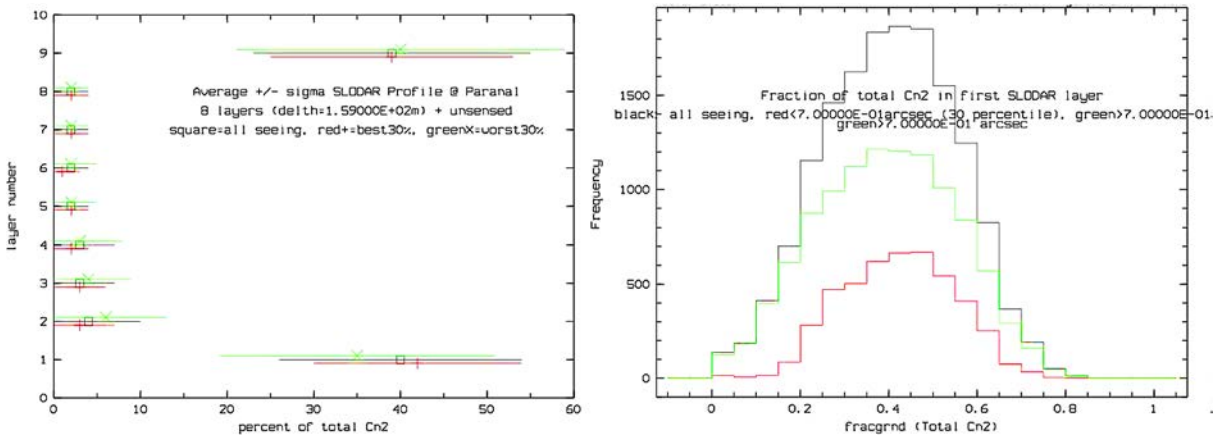

Fig. 2. Right: preliminary turbulence profile statistics; Left: fraction of turbulence located at 200 m (Paranal).

From this analysis, the potential interest of combining wavefront sensing tomography with one DM conjugated to the ground was proposed (Rigaut [11]). This is what we call Ground Layer Adaptive Optics (GLAO); see Fig. 1. It aims at improving the seeing over a field of view much larger than the isoplanatic angle patch size, with a uniform correction quality over the entire corrected field.

Later MASS was tested on sky and provided its first high altitude C_n^2 profiles (Kornilov [13]). MASS measurements were then combined with DIMM measurements to determine the boundary layer of the turbulence by difference of the integral seeing measured by DIMM and of the high layers seeing measured by MASS – MASS does not detect the turbulence to the ground because it measures scintillation. Finally, the altitude resolution of MASS being too low to accurately determine the exact structure of the boundary layer – over the first two kilometres –, the SLOpe Detection and Ranging system (SLODAR) was developed in collaboration with University of Durham (Wilson [14]). The combination of DIMM-MASS, and the SLODAR is ideal for the long term statistical study of the turbulence profile at a given site and more specifically for the determination of the performance of a GLAO system.

2. Ground layer and C_n^2 profiles

Preliminary measurements made at Paranal in 2003 with MASS-DIMM showed that the boundary layer was contributing for at least 60% of the total turbulence. More recent measurements of the turbulence profile (C_n^2) made at Paranal with the SLODAR and DIMM-MASS have shown that 60% of the turbulence is located within the first two kilometres and that 40% of the turbulence is concentrated at 200 m; see Fig. 2.

These preliminary C_n^2 results confirm there is the potential for improving significantly the image quality by correcting the main turbulence layer over a large FoV.

3. Context, input parameters and trade-off

The AO system model is provided in Le Louarn [15] and the details about the GLAO performance in the visible and in the IR are respectively described in Le Louarn et al. [16,17].

The GLAO performance in the visible have been computed for the Ground Atmospheric Layer Adaptive Corrector for Spectroscopic Imaging – GALACSI –. GALACSI aims at concentrating the energy of a Point Spread Function (PSF) over a $1'$ FoV for a visible-light (450–930 nm) integral field spectrograph. This system is designed to feed the Multi Unit Spectrographic Explorer (MUSE), a second generation instrument for the European Southern Observatory (ESO) Very Large Telescope (VLT), (Bacon [18]) and (Henault et al. [19]).

The GLAO performance in the near infrared has been computed for the Ground layer Adaptive optics Assisted by Laser –GRAAL. GRAAL aims at concentrating the energy of a PSF over a $10'$ FoV for a Near IR imager. This system is designed to feed the High Acuity Wide field K-band Imaging – HAWK-I –, an instrument for the ESO VLT, (Pirard et al. [20]).

Both GALACSI and GRAAL are based on multi-sodium-LGS with a brightness of typically magnitude 9 located at fixed and optimal positions. Moreover, they are monochromatic, and therefore their scattered light is easier to filter out than the light from NGSs which is especially important for deep-field 3D spectrography.

Several reasons have motivated the multi-sodium LGS tomography approach as compared to the multi-NGSs or multi-LGSs Rayleigh concepts (Le Louarn et al. [16,17]):

- The VLT diameter of 8 m.
- The 3D Ultra Deep Field science of MUSE calls for very long integration time – 80 hours – leading to take 70% percentile of the seeing statistics at Paranal: 1.1″ seeing at 0.5 μm with a zenith angle of 30°. This implies high guide star fluxes because of the required small sub-apertures.
- The visible wavelength of MUSE: 750 nm, implying small sub-apertures, i.e. high flux from the guide stars.
- The science deep fields to be observed with MUSE are very close to the Galactic Pole where bright enough reference stars are scarce.
- The so-called 'narrow field' mode of MUSE at 650 nm which aims at diffraction limited imaging. Its small field of view (∼3″) and high performance requirements (∼10% of Strehl at 650 nm) is incompatible with the use of multi-NGS.
- The 10′ FOV required for HAWK-I.

There are of course some fundamental limitations of multi LGS based systems like the indetermination of the Tip-Tilt (TT) from the individual LGSs (Foy [21]), the LGS spot elongation (Viard et al. [22]) and to a lesser extend the filtering of the Rayleigh light which is much more intense than the sodium guide star itself.

We shall neglect the LGS spot elongation and scattered light problems at this stage. The spot elongation is of moderate importance on an 8-m class telescope, as shown by (Viard et al. [22]). However, if each LGS is projected from the side of the telescope instead of being projected from behind the secondary mirror, a reduction of the AO performance is expected which can be retrieved by increasing the laser power (Ellerbroek [23]). Note that the side LGS launching scheme has two main advantages:

- Reduce the Rayleigh scattering in the science FoV.
- Avoid the so-called 'fratricide effect' between wavefront sensors when CW laser are used: certain sub-apertures of WFS-1 collect the Rayleigh scattered light of the LGS-2 on top of the sodium light of the LGS-1. This Rayleigh light is equivalent to a sky background for the considered sub-apertures but its variability during the observation makes its subtractions inaccurate leading to a higher noise.

In the following, a four sodium-LGS configuration will be selected. Each LGS wavefront is measured by a 30×30 sub-aperture Shack Hartmann WFS. The high spatial wavefront sampling is required because of the severe atmospheric conditions assumed and the scientific observing wavelength for GALACSI (this number is driven by the narrow field mode). For the purpose of WFS standardisation the same spatial sampling will be assumed for GRAAL although it has been demonstrated that the number of sub-apertures can be relaxed to 20×20 sub-apertures – or less – in that case without loosing in Ensquared Energy (EE) (Le Louarn and Hubin [17]). We assumed a RON of the detector of 3 e-rms and 8×8 pixel/sub-aperture for centroid calculations.

The LGSs are organised in a square geometry at 70″ off axis for GALACSI and at 5′ off-axis for GRAAL (see Fig. 4). LGSs are focused at 90 km above the telescope. They are therefore outside the scientific FoV both for GALACSI and GRAAL which makes easier to filter out in the science path (MUSE) and avoid the vignetting of the science FoV with the WFS pick-up arm for HAWK-I. In the case of GALACSI, the four LGSs can be reconfigured in a square pattern of 30″ diagonal. In this so-called Laser Tomography Adaptive Optics (LTAO) or narrow field mode, the correction is optimised on-axis and the four LGSs are essentially used to overcome the cone effect limiting the performance of one LGS in the visible.

The GLAO performance are numerically simulated by propagation of phase screens temporally shifted. The propagated phase screens are cut into pieces (each piece corresponding to a WFS sub-aperture) and a Fourier transform is made to compute the spot shape in each sub-aperture. The centroid is then computed and the x and y sloped are the WFS outputs. The command matrix uses an average of the measurements obtained from each WFSs providing a very uniform correction over the corrected FoV. Although the command seems quite primitive, it has been shown (Rigaut [11]) that the performance obtained is acceptable both in term of EE and PSF uniformity. After multiplication by a command matrix, the command is applied to the Deformable Mirror DM conjugated close to the ground. The DM is then shaped accordingly and the residual wavefront is computed. After one temporal step of the phase screen temporal the new wavefront is computed. Each simulation step is 2 ms. In the following simulation results two frames delay have been assumed.

The PSF is computed in any point in the corrected FoV by making the Fourier transform of the residual phase in that direction to get a short exposure PSF at each temporal step. A long exposure PSF consists of an average of 5000 short exposure PSFs.

It has been shown (Le Louarn and Tallon [24]); (Ellerbroek and Rigaut [25]) that, in the general MCAO case, the indetermination of the Tip-Tilt (TT) from multiple LGSs leads to an indetermination of defocus and astigmatism when several DMs are used. Recent work from (Lloyd-Hart and Milton [26]); (Le Louarn and Hubin [16]) have shown that, in the case of one DM, this degeneracy is not present and a single TT NGS is required. This can be explained by the fact that the tip-tilt produced by the ground atmospheric layer is corrected by an off-axis NGS: anisoplanatism in that case is large. The rest of the tip-tilt is

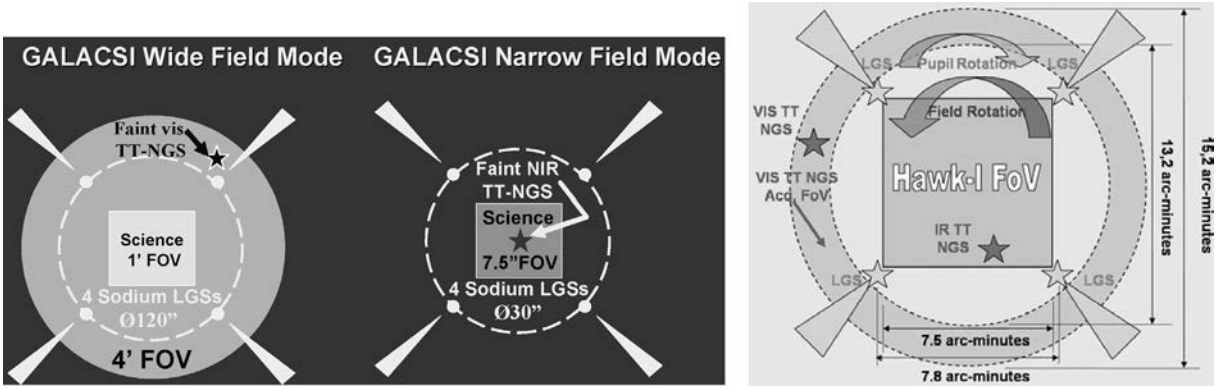

Fig. 3. Multi-LGSs and Tip-tilt NGS configuration for GALACSI-MUSE in the Wide (left), Narrow (middle) Field modes and for GRAAL (right).

Fig. 4. Left: gain in Ensquared Energy in 0.2″ versus wavelength; Middle: same for 30% worst seeing; Right: same for 30% best seeing.

wrongly measured by this off-axis NGS but its variance and its impact on the ensquared Energy performance is small. In return, the stability of the PSF FWHM over the FoV is probably affected and would require three tip-tilt NGSs.

4. Performance and simulations

Performance simulations have been conducted based on the concept, trade-off and assumptions presented on the previous section.

Fig. 4 provides the gain in Ensquared Energy (EE) in a pixel of 0.2″ for GALACSI versus the observing wavelength based on recent C_n^2 profiles measured at Paranal. These profiles, obtained over 20 nights, do not represent a long term statistic of the site and therefore the resulting performance should be taken with care. The results show a gain in EE of about 1.8 at 750 nm for all the seeing considered (left curve). We see also that the gain is higher in the case of worst seeing (mid curve) than in the case of good seeing (right curve). In case of 'bad' seeing the amount of ground turbulence seems to be higher than in the 'good' seeing case. Based of these results, we can conclude that a GLAO system is not only a 'seeing reducer' but also a 'seeing stabilizer': GLAO essentially improves the proportion of 'good' seeing for the site which means better PSF stability versus time.

Fig. 5 provides the gain in Ensquared Energy in a pixel of 0.1″ for GRAAL versus the off-axis angle for the K-band. The average gain in EE is above 2 for all seeing cases. The PSF uniformity is quite good over the whole 10′ FoV. As for GALACSI the gain is higher for the 'bad' seeing case than for the 'good' seeing case.

Based on the above results we can conclude that a gain in EE of 1.8 to 2.5 is achievable with a GLAO system at both IR and visible wavelengths. A factor 2 of EE translates into a factor 2 of integration time and therefore a factor 2 of telescope time! Assuming 100 observing nights/year and a lifetime of HAWK-I with GRAAL of 10 years, the gain of telescope time amounts to 500 nights corresponding to 25 M€ (Operation of one VLT unit telescope is about 50 k€/night).

A factor 2 of EE can also be translated into a factor 2 of telescope collecting area – corresponding to a telescope diameter of 11 m – or to a gain of 0.5 magnitude in depth for the Galaxy evolution surveys – corresponding to a gain in distance of 1.26.

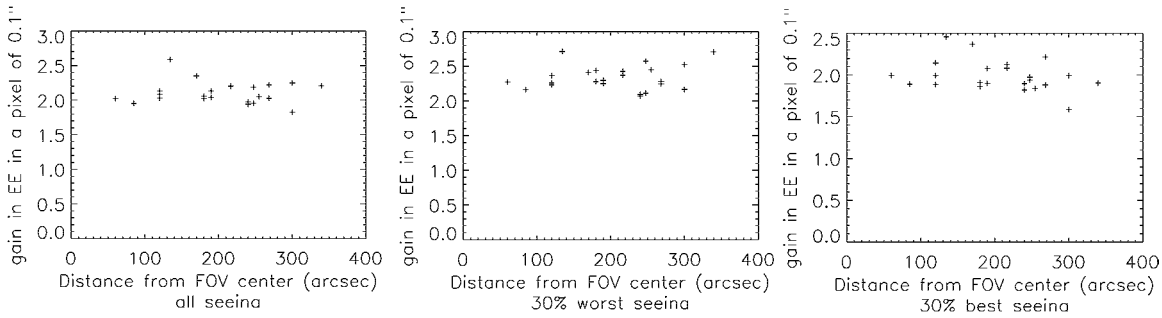

Fig. 5. Left: ensquared Energy gain in 0.1″ vs. off-axis angle; Middle: 30% worst seeing; Right: 30% best seeing.

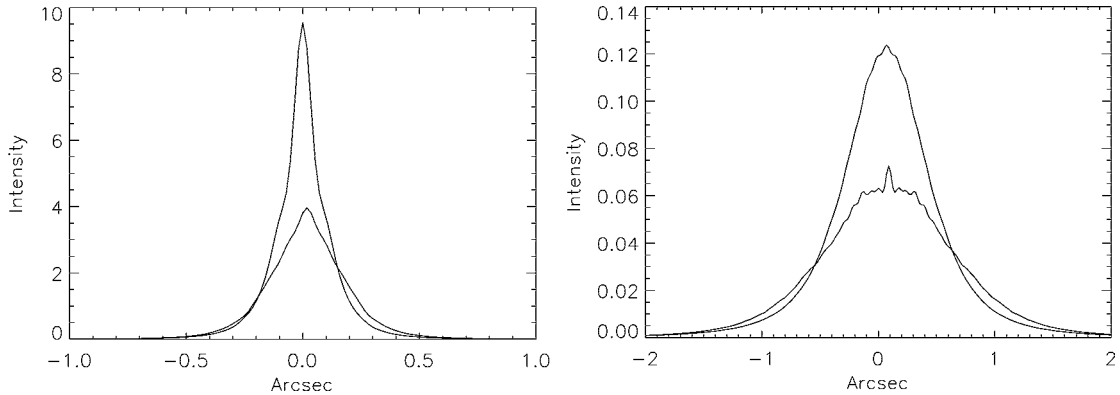

Fig. 6. Left: K-band corrected/uncorrected PSF profiles with GRAAL; Right: 750 nm corrected/uncorrected PSF profiles with GALACSI. Good Seeing.

The PSF uniformity over the corrected FoV – not the case of normal AO system – is also very valuable for the astronomical programs expected to be conducted with GLAO. The PSF shape is comparable to the well-known seeing limited PSF with a better FWHM as shown in Fig. 5. The "seeing stabilizer" capability of GLAO is also important as it guaranties a better PSF stability over a given period of time and a better predictability of the performance.

Fig. 6 provides the corrected and uncorrected PSF profiles both for GRAAL and GALACSI.

5. Practical implementation of GLAO: GALACSI and GRAAL cases

As discussed in the performance evaluation section, the major advantage of implementing a GLAO system is to improve the EE by a factor of 2. Consequently, the basic objective of any GLAO system should be to maximize the throughput toward the focal plane instrument and to maintain this gain as high as possible.

Adaptive Optics designs developed up to now have been limited in FoV – typically 1–2′ – and based on 5–7 optical reflections before entering the scientific instrument. This translates to a transmission loss of about 20% at best – assuming an excellent dichroic/Notch filter sharing the light between the wavefront sensor and the instrument. In addition, designing a post-focal AO system with 10′ is extremely challenging, not photon effective and costly.

For these reasons, we have decided to base our GLAO system design on the availability at the VLT of a Deformable Secondary Mirror (DSM). This eliminates all the relay optics required to re-image the pupil on the deformable and Tip-tilt mirrors and to produce the image plane to the instrument. The corrected FoV can be as large as the telescope FoV; the instrument background is limited to the telescope background.

The other key feature of a GLAO design is to spatially separate the corrected scientific FoV from the FoV required for the wavefront sensor sources. This is relatively easy to achieve with multi-Laser Guide Stars since they can be located and fixed outside the science FoV.

This baseline provides 100% throughput to the instrument and easily allows for observation without AO – when required – as soon as the shape of the DSM can be maintained in active mode.

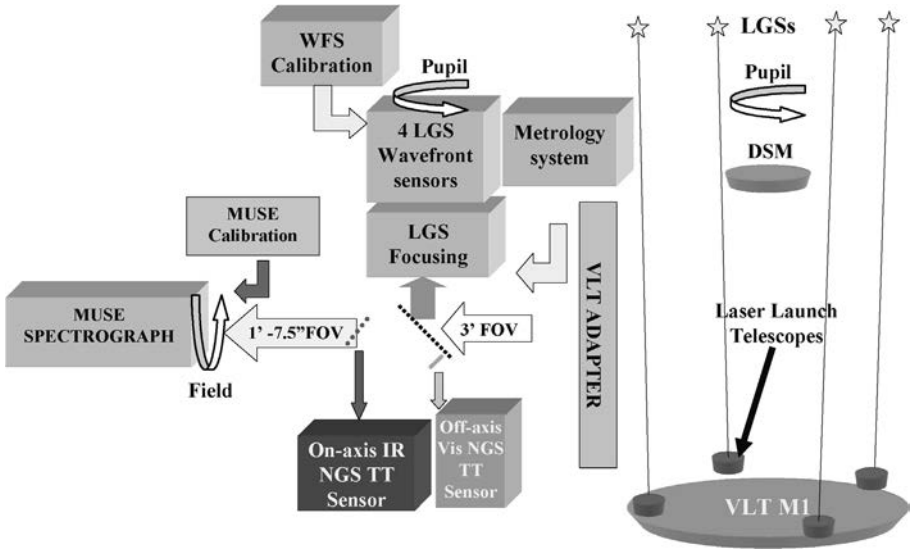

Fig. 7. GALACSI concept.

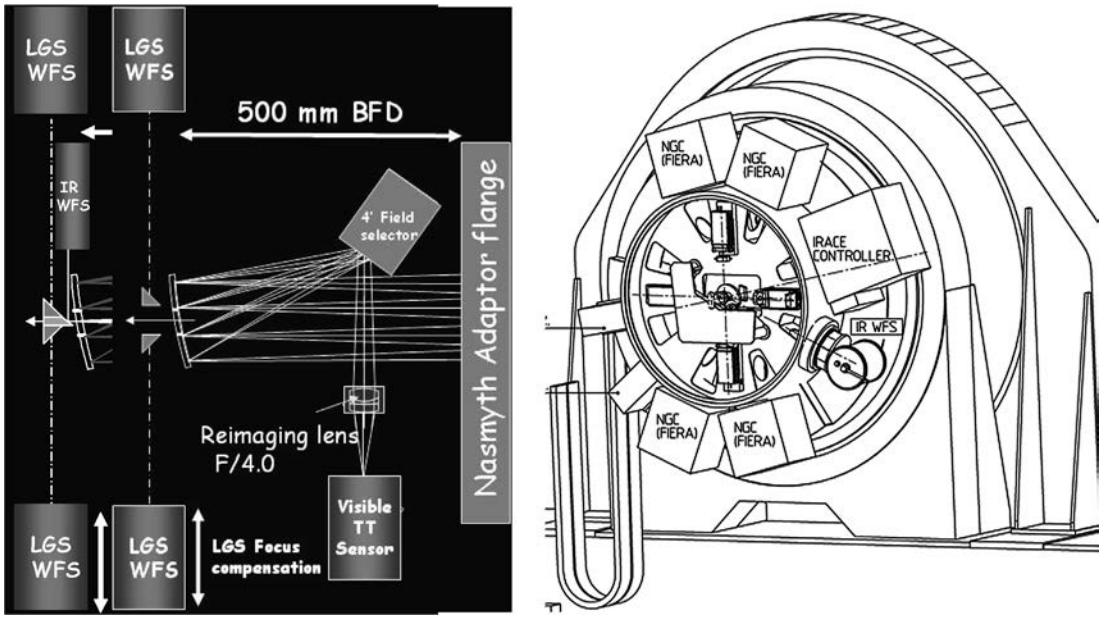

Fig. 8. Left: Optical design of GALACSI in narrow field mode, (middle) optical design of GALACSI in wide Field mode; Right: mechanical implementation of GALACSI at VLT Nasmyth Focus.

Fig. 7 provides the concept for GALACSI and Fig. 8 shows the corresponding optical concept and mechanical implementation. The GALACSI concept can be summarised as follows:

1. GALACSI is at the Nasmyth focus of one VLT with a back focal distance of 500 mm at F/15.
2. Four Sodium Laser Guide Stars arranged in a square configuration and emitted from four 50 cm laser projectors located on the VLT centrepiece ring. The four lasers are emitted toward the centre of the scientific FOV such that to avoid Rayleigh scattered light crossing the visible scientific FOV and therefore limit the light-scattering. Sodium LGS are reconfigurable such that to fulfil both the $1'$ and the LTAO or Narrow FoV needs. The expected return flux from a single Sodium Laser Guide Star is 2.5×10^6 Na photons/m^2/s (goal 5×10^6).

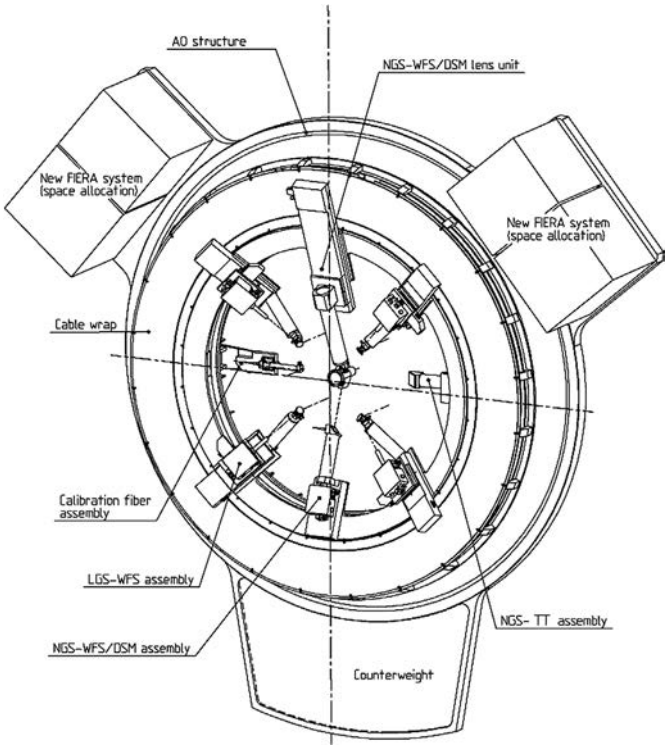

Fig. 9. Opto-mechanical concept of GRAAL.

3. Since the LGS are attached to the primary mirror cell structure, the sodium laser spots rotate like the pupil at the Nasmyth focal plane of the VLT. Therefore the 4 WFSs should rotate like the telescope pupil to follow the laser images.
4. Altitude of the LGS reference stars varies with the altitude of the mesospheric sodium atoms altitude and with the telescope zenith angle. Assuming a maximum zenith angle of 60 degrees the variation of the telescope-laser spot varies from 80 to 180 km. This corresponds respectively to a defocus of 180 and 80 mm at the VLT Nasmyth focus (F/15). The LGS WFSs are designed to acquire and track the focus of the corresponding laser spots.
5. The light from the LGSs is transmitted to the WFSs while the tip-tilt NGS light is reflected by the Sodium dichroic toward Tip-tilt sensor via a field selector scanning a $4'$ annular FoV – the central $1'$ is reserved for the science FoV and is free of any optical surface. The expected limiting magnitude of the NGS Tip-tilt is $Mv = 18$. The expected sky coverage has been studied for GALACSI (Stuik et al. [27]) and 80% sky coverage at the Galactic pole is achievable with a search FoV of $4'$.

For the Narrow Field mode an on-axis IR tip-tilt Natural Guide Star sensor will be used. Light separation will be done with a VIS/IR dichroic located before the Adaptive Optics focal plane.

Fig. 9 provides the opto-mechanical design of GRAAL which can be summarised as follows:

1. GRAAL is at the Nasmyth focus of one VLT with a back focal distance of 250 mm at F/15.
2. Four Sodium Laser Guide Stars as for GALACSI but located at in a square of about $8'$ and rotating like the pupil. The LGS WFSs are designed to acquire and track the focus of the laser spots.
3. The light from the LGSs are directed to the WFSs by pick-up mirrors. The tip-tilt NGS light is acquired by a separate pick-up arm patrolling the annular FoV [13–$15'$] outside the science FoV. The expected limiting magnitude of the NGS Tip-tilt is $Mv = 18$.
4. An additional wavefront sensor has been implemented to permit the commissioning of the VLT Deformable Secondary Mirror on-axis. A re-imaging objective provides the Nyquist sampling n K-Band to the HAWK-I instrument.

6. Deformable secondary mirror for the VLT

As described in the previous section Deformable Secondary Mirror (DSM) is an essential component of a Ground Layer Adaptive Optics system permitting essentially to transmit 100% of the science objects light (Arsenault et al. [28]) and (Hu-

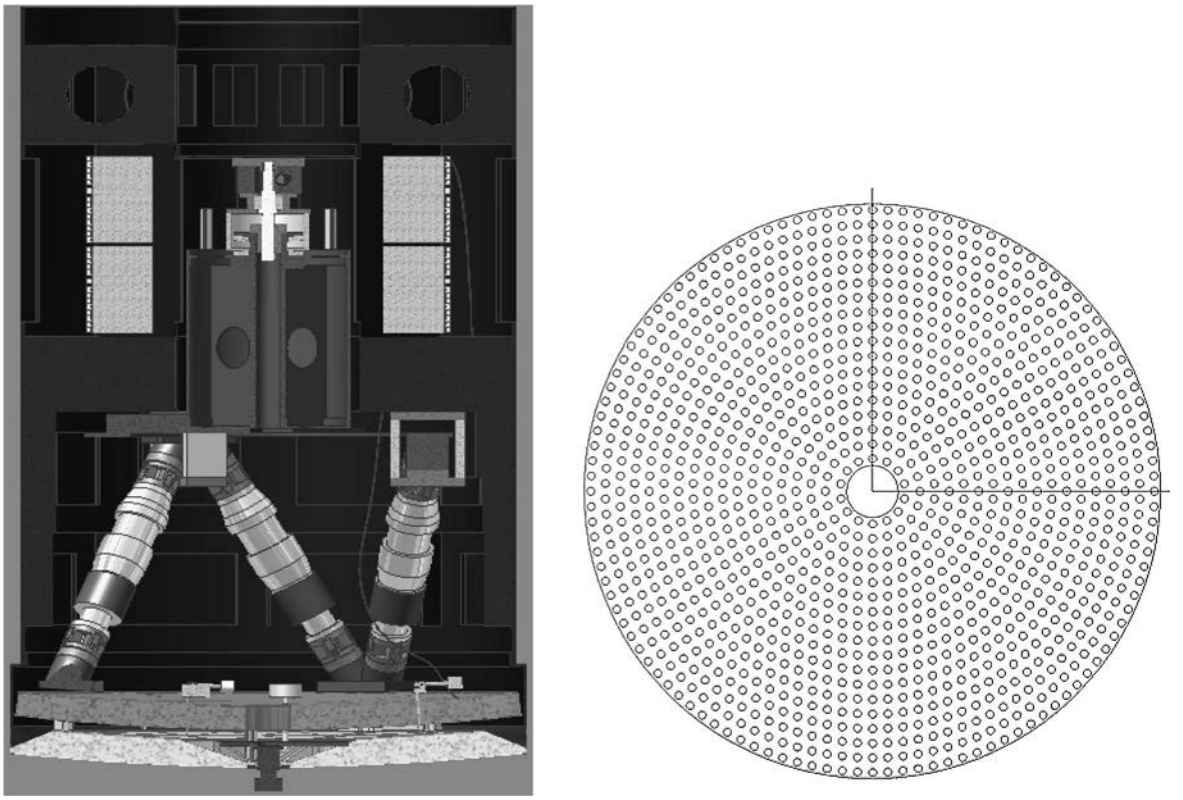

Fig. 10. Left: VLT Deformable Secondary Mirror concept; Right: actuator pattern (Courtesy Microgate, ADS and INAF Arcetri).

bin [29]). For the VLT a conceptual design of 1170 actuators DSM has been developed by Microgate-ADS in collaboration with INAF-Arcetri in Italy – Fig. 10. The concept of the DSM is derived from the Large Binocular Telescope adaptive secondary design (Riccardi et al. [30], Gallieni et al. [31]).

The concept is based on the deformation of a thin Zerodur shell controlled by a pattern of electromagnetic actuators. Each actuator is made of a fixed coil and a moving magnet glued on the back of the shell. The coil is mounted on an aluminium cold finger providing the structure of the actuator and the heat sinking of the coil. The actuator cold fingers are mounted on an aluminium disk – cold plate – liquid cooled. A back-plate inserted between the thin shell and the cold plate, provides a stable optical reference to the thin shell. Capacitive sensors are co-located to each actuator to measure the distance between the back-plate and the thin shell. The current of each actuator voice coil motor is controlled by a digital loop using the information provided by the capacitive sensors. A set of specialised DSPs control in real time the shape of the thin shell according to the command received from the AO Real Time Computer. The DSM concept is therefore based on force actuators with a local controlled loop which guarantees the shape of the shell at any time.

The tuning of Deformable Secondary Mirror and Ground Layer Adaptive Optics using multi-laser tomography is definitely a complex task. To avoid long and painful commissioning at the telescope, it is essential to develop a laboratory test facility simulating the four Laser guide stars, the multi-layer atmosphere over a representative FoV and the telescope with the Deformable Secondary Mirror – Fig. 11. The proposed concept is based on a 1.6 m aspheric mirror and allows closed loop testing on-axis with NGS. A 3D turbulence generator using phase screens and a field corrector allows the GLAO testing with multi-LGSs up to a FoV of 3–4′. An output F/15 optical beam is provided for the installation and testing of GALACSI or GRAAL.

7. From Ground Layer to laser Tomography AO

As discussed previously Ground Layer AO is essentially a seeing reducer over a large FoV and therefore the correction provided remains low. To improve this correction, one can reduce the size of the square pattern of the sodium laser spots such as to probe the column of turbulence above the telescope – and avoid the usual cone effect – and have enough overlap of the meta-pupils at 8–10 km. An on-axis optimum wavefront can then be reconstructed and applied to one deformable mirror

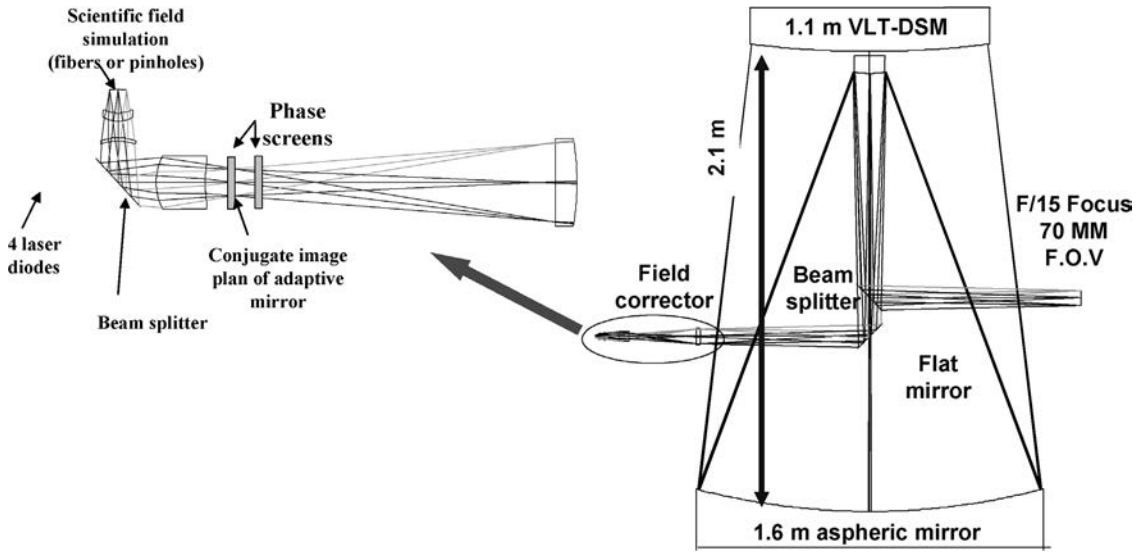

Fig. 11. GLAO-DSM test facility concept.

Table 1
Simulation parameters assumed for the Laser Tomography Mode of GALACSI

Parameter	Value
Number of sub apertures–active actuators	32×32–881
Number–position of LGSs–Position of NGS	4–15″ off-axis–on-axis
LGSs – Tip-tilt NGS flux	360–1000 ph/sub aperture/frame
Frame rate/delay/loop gain	700 Hz/2 frame/0.5
Wavelength–Seeing–τ_0	0.75 μm–0.65″–3 ms

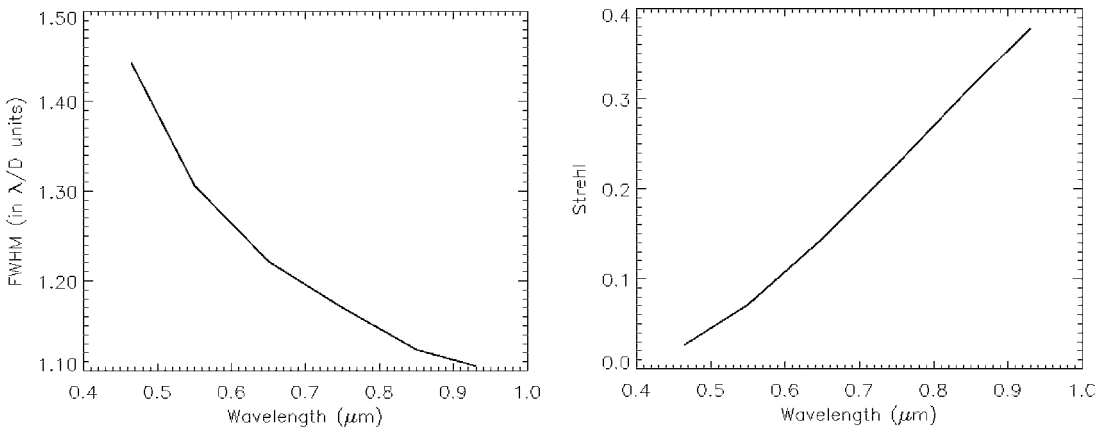

Fig. 12. GALACSI Performance in Narrow Field Mode. Left: FWHM vs. wavelengths λ/D; Right: Strehl vs. wavelength.

conjugated to the ground or at low altitude. This concept is called Laser Tomography Adaptive Optics and is able to provide a good correction at short wavelength with reasonable sky coverage – a Natural Guide Star is still required to measure the individual Laser tip-tilts. This concept is the so-called narrow field mode of GALACSI.

Table 1 provides the simulation parameters assumed for the Laser Tomography Mode of GALACSI.

Fig. 12 shows the Narrow Field Mode FWHM performance as a function of wavelength and the Strehl curve as a function of wavelength. Strehl variation from 10% (in the blue) to almost 40% near 1 μm are shown. The instrumental error budget as well as LGS spot elongation and Na height variations have been neglected here. Based on our experience with the first generation of

AO systems, we are confident that an error budget error of 80 nm rms can be achieved: for instance Strehl ratios of 95% in K (79 nm rms) have been obtained with the MACAO system in closed loop without turbulence. 80 nm rms corresponds to about Sr(650 nm) = 0.55 leading to reduce the simulated Strehl by a factor 2 at this wavelength.

In the Laser Tomography Mode the guide star has to be within the science field, which has a size of $7.5'' \times 7.5''$ and therefore NIR counterpart of the on-axis object itself must be use for tip-tilt sensing.

8. Conclusions

We have introduced the concept of Ground Layer Adaptive Optics and underlined the advantages of such concept for astronomy. Two applications of this concept have been presented: GALACSI and GRAAL respectively for medium FoV correction in the visible and large FoV correction in the NIR. GALACSI and GRAAL conceptual designs have been given and expected performance have been presented. The attractive Deformable Secondary Mirror concept for GLAO systems has been shown. Extensions of the GLAO concept to Laser tomography and the corresponding performance have been given.

Acknowledgements

Part of this work is funded by the Optical Infrared Co-ordination Network for Astronomy (OPTICON) funded by the European Commissions 6th Framework programme under contract number RII3-Ct-2004-001566. The authors would like to thank R. Bacon for the numerous interactions necessary to converge to GALACSI for MUSE, Marc Sarazin for his help in choosing the atmospheric model used in this paper, Daniele Gallieni, Roberto Biasi and Armando Riccardi for the conceptual design of the VLT DSM.

References

[1] R. Foy, A. Labeyrie, Astron. Astrophys. 152 (2) (1985) L29–L31.
[2] M. Tallon, R. Foy, Astron. Astrophys. 235 (1990) 549–557.
[3] J. Beckers, in: Very Large Telescopes and their Instrumentation, ESO, 1988, p. 693.
[4] B.L. Ellerbroek, J. Opt. Soc. Am. A 11 (2) (1994) 783.
[5] D.C. Johnston, B.M. Welsh, J. Opt. Soc. Am. A 11 (1) (1994) 394.
[6] R. Ragazzoni, E. Marchetti, F. Rigaut, Astron. Astrophys. 342 (1999) L53–L56.
[7] A. Tokovinin, M. Le Louarn, M. Sarazin, J. Opt. Soc. Am. A 17 (10) (2000) 1819–1827.
[8] B. Ellerbroek, et al., in: Proc. SPIE, vol. 4839, 2003, pp. 55–66.
[9] J. Vernin, C. Munoz-Tunon, Astron. Astrophys. 284 (1994) 311–318.
[10] M. Le Louarn, N. Hubin, M. Sarazin, A. Tokovinin, Mon. Not. R. Astron. Soc. 317 (3) (2000) 535–544.
[11] F. Rigaut, in: E. Vernet, R. Ragazzoni, S. Esposito, N. Hubin (Eds.), Beyond Conventional Adaptive Optics, ESO, 2002; M. Tallon, R. Foy, Astron. Astrophys. 235 (1–2) (1990) 549–557.
[12] A. Tokovinin, V. Kornilov, in: J. Vernin, Z. Benkhaldoun, C. Muñoz-Tuñón (Eds.), in: ASP, vol. 266, 2002.
[13] V. Kornilov, et al., in: Proc. SPIE, vol. 4839, 2003, pp. 837–845.
[14] R.W. Wilson, et al., in: Proc. SPIE, vol. 5490, 2004, pp. 758–765.
[15] M. Le Louarn, Mon. Not. R. Astron. Soc. 334 (2002) 865.
[16] M. Le Louarn, N. Hubin, Mon. Not. R. Astron. Soc. 349 (3) (2004) 1009–1018.
[17] M. Le Louarn, N. Hubin, Mon. Not. R. Astron. Soc. (2005), submitted for publication.
[18] R. Bacon, et al., in: Proc. SPIE, vol. 5492, 2004, pp. 1145–1149.
[19] F. Henault, et al., in: Proc. SPIE, vol. 5492, 2004, pp. 909–920.
[20] J.F. Pirard, et al., in: Proc. SPIE, vol. 5492, 2004, pp. 1763–1772.
[21] R. Foy, Laser Guide Star Adaptive Optics for Astronomy, NATO ASI, Kluwer Academic Publishers, 1999, p. 25.
[22] E. Viard, F. Delplancke, N. Hubin, N. Ageorge, in: R.K. Tyson, R.Q. Fugate (Eds.), in: Proc. SPIE, vol. 3762, 1999.
[23] B. Ellerbroek, in: Proc. SPIE, vol. 5382, 2004, pp. 478–489.
[24] M. Le Louarn, M. Tallon, J. Opt. Soc. Am. A 19 (2002) 912.
[25] B.L. Ellerbroek, F. Rigaut, J. Opt. Soc. Am. A 18 (2001) 2539.
[26] M. Llyod-Hart, N.M. Milton, J. Opt. Soc. Am. A 20 (2003) 1949.
[27] R. Stuik, in: Proc. SPIE, vol. 5490, 2004.
[28] R. Arsenault, et al., ESO Messenger N^{o} 115, 2004.
[29] N. Hubin, in: Proc. SPIE, vol. 5490, 2004.
[30] A. Riccardi, et al., in: Proc. SPIE, vol. 5490, 2004.
[31] D. Gallieni, et al., in: Proc. SPIE, vol. 5490, 2004.